Chromatographia (2012) 75:661–670
DOI 10.1007/s10337-012-2240-6

ORIGINAL

CZE of Sulfur-Containing Amino Acids and Peptides and Its Application to the Quantitative Study of Heavy Metal-Caused Thiol Oxidations

Anne-Christine Schmidt · Stefanie Lauckner · Katja Lindner

Received: 6 January 2012 / Revised: 14 March 2012 / Accepted: 3 April 2012 / Published online: 22 April 2012

Abstract The redox-active, sulfur-containing amino acids cysteine and methionine, the tripeptide glutathione and their oxidized counterparts cystine, methionine sulfoxide, and glutathione disulfide were separated as anions by capillary zone electrophoresis (CZE) in a 72 cm long fused silica capillary filled with 100 mM phosphate buffer, pH 8.0, at a voltage of +30 kV in 20 min. The optimized CZE method was suited for the implementation of quantitative metal interaction studies of the biomolecules in a biologically relevant concentration range (μM–mM). Decreasing peak areas of the reduced forms of cysteine and glutathione and simultaneously increasing peak areas of the oxidized forms after incubation of the reduced biomolecules with divalent heavy metal cations indicated redox reactions which could be responsible for toxic metal actions in biological systems. CZE measurements revealed that a 50 % oxidation grade of cysteine was achieved at a molar metal:cysteine ratio of 0.85 in case of Zn(II) addition and of 0.11 in case of Cu(II) addition, respectively. Cu(II) oxidized 50 % of the initial glutathione at a molar Cu:peptide ratio of 0.036, whereas the 50 % oxidation grade was not reached after incubation with Co(II) up to a molar ratio of Co:peptide of 0.25.

Keywords Capillary zone electrophoresis · Cysteine · Glutathione · Thiol oxidation · Heavy metals

A.-C. Schmidt (✉) · S. Lauckner · K. Lindner
Institute of Analytical Chemistry, Technical University Bergakademie Freiberg, Leipziger Straße 29, 09599 Freiberg, Germany
e-mail: Anne-Christine.Schmidt@chemie.tu-freiberg.de

Introduction

The contents of the sulfur-containing amino acids cysteine (Cys) and methionine (Met), of the small peptide glutathione (γ-Glu-Cys-Gly; GSH) and their oxidized dimeric forms cystine (Cys–Cys) and glutathione disulfide (GSSG) in biological fluids serve as indicators for various diseases [1–4]. The redox-active tripeptide glutathione is significantly involved in the cellular redox regulation and counteracts oxidative stress. GSH belongs to the most prevailing thiol compounds in plant and animal cells. In human liver cells and red blood cells, GSH concentrations of 7.5 mM [5] and 3 mM [6], respectively, appear, whereas 0.2–0.5 mM cysteine concentrations are found in hepatocytes [7]. Further, GSH serves as precursor for the biosynthesis of metal-chelating polypeptides involved in metal detoxification and homeostasis [8]. Instead of a direct binding, metal ions characterized by a large oxidation potential, such as Cu(II) oxidize GSH to GSSG [9]. A large number of studies demonstrated that the GSH/GSSG ratio can be considered as a reliable index of the cellular redox state.

Liquid chromatographic (LC) and capillary electrophoretic (CE) methods are most widely used to differentiate biological thiol compounds and their disulfides in different sample types [1–4, 10–12]. The suitability of capillary zone electrophoresis (CZE) for the analysis of amino acids and peptides, in general, is demonstrated in current reviews [13, 14]. Also larger thiolic peptides, such as different types of phytochelatines, can be separated by means of CZE [15]. Minimal sample, reagent and solvent consumptions, low instrumental and operational costs, high separation efficiencies, and short analysis times pertain to the advantages of CE-based measurements. A smaller susceptibility to irreversible modifications of the capillaries

caused by sample constituents in comparison to LC columns is also emphasized [16]. A reduction of sample preparation and electrophoretic separation on a microchip format to enable the analysis of intracellular sulfhydryl compounds in single cells is presented in [17]. To analyze thiol compounds from real biological samples in a larger scale, an enrichment step using solid phase extraction cartridges was inserted in the sample preparation procedure [15]. Since biological thiol compounds are existent as anions at pH >7, CZE separations were primarily performed in an alkaline buffer medium. For example, four low-molar mass thiols (homocysteine, cysteine, glutathione, and *N*-acetylcysteine) were separated in the CZE mode using 20 mM phosphate running buffer, pH 7.8 [1]. Four sulfur-containing amino acids including L-cysteine, L-cystine, DL-homocystine, and L-methionine were studied in a 70 cm long × 75 µm i.d. fused silica capillary filled with 10 mM disodium tetraborate buffer, pH 9.8 [18]. The oxidized and the reduced form of glutathione were analyzed under similar conditions in an uncoated 37 cm × 75 µm capillary with a 300 mM borate buffer, pH 7.8 [3]. Glutathione, glutathione disulfide, cysteine, cystine, homocysteine, homocystine and the therapeutic agents penicillamine, penicillamine disulfide, *N*-acetylcysteine, and captopril could be separated as anions in 0.01 M phosphate buffer, pH 7.4, as well as in cationic form in 0.1 M phosphate buffer, pH 2.3 [10].

Because of a low concentration sensitivity of the common UV detection for LC- and CE-separated amino acids and peptides, more complicated detectors, such as microelectrodes [1] or a coupling to elemental mass spectrometry [18] or to electrospray ionization mass spectrometry [19], were employed to improve the detection capability. Another experimental strategy to enhance the detection sensitivity consists in the derivatization of the thiol groups by chromophoric or fluorophoric agents [2, 10, 20]. Recent reviews focused on sensitivity-improving derivatizations for UV and fluorescence detection of biological thiols separated by LC or CE, various derivatization reagents are listed [12, 16]. Because such approaches involve reductive conversions of disulfidic forms to enable reaction with the chromophores, the possibility to analyze reduced and oxidized species in parallel is strongly constrained. Moreover, a risk for a thiol-disulfide interconversion exists during the derivatization procedure [4] distorting the original redox state of the analytes and the derivatization yields must be considered [2]. Also regarding a detection of possible metal bindings, a derivatization procedure proves to be inappropriate because metal-sulfur coordinations must be broken prior to reduction and subsequent reaction with the derivatization agent [20]. Problems occurring in case of quantitative disulfide determination by the way of subtraction of the original reduced thiol content from the total content reflected by the sum of the original reduced thiol content and the content of the reduced disulfide are discussed in [12]. The author of this review recommends a simultaneous determination of both the thiol and the corresponding disulfide in order to afford a detailed functional resolution of thiolic and disulfidic metabolites.

In the current study, a CZE separation method was developed for six low-molar mass sulfur-containing biomolecules comprising the reduced and oxidized forms of the amino acids cysteine and methionine, and of the tripeptide glutathione. This non-elaborate method could be successfully applied for the quantitative analysis of heavy metal influences on the redox state of the important redox-regulating biomolecules. The presented work contains, to our knowledge, the first CZE-based approach for the study of metal effects on biological thiols. The considered analytes have not been investigated in this combination by existing CE methods. Some of published studies dealing with biological thiol analysis are restricted to the reduced forms whereas the oxidized counterparts were not detected [1, 11, 15, 17]. Other CE methods are focused either on glutathione-related analytes [3], on amino acids [18], or on glutathione and cysteine in combination with aromatic amino acids [4]. A large part of the established methods involves the above-mentioned labeling with a UV- or fluorescence active marker implying a reductive conversion of disulfidic forms [2, 11, 12, 15, 16]. Regarding the elucidation of metal interactions, such a reductive labeling procedure contains an unknown interference of the back-reduction step with the equilibrium of the metal-induced thiol oxidations. In order to improve the sensitivity of the UV detection in the current work, a capillary with an extended light path named bubble cell was employed. Sensitivity enhancement has been achieved in CZE-UV using such capillaries for bioanalytical purposes [21, 22]. Since physiological conditions should be approximated to implement the metal–biomolecule interaction studies, CZE separations of biological thiols in an acidic [4, 10] or alkaline [17] pH range should be avoided. Moreover, higher proton activities compete with metal cations for reaction sites of biomolecules [9]. In the presented method development, a compromise between an about neutral pH value in the separation medium and a high separation power should be found.

Materials and Methods

Chemicals

The sulfur-containing amino acids and peptides L-cysteine (Cys), L-methionine (Met), L-cystine (Cys–Cys), DL-methionine sulfoxide (MetSO), L-glutathione (GSH),

and L-glutathione disulfide (GSSG) were purchased as solid substances in a purity grade of >98 or >99 % from Acros Organics, Geel, Belgium. 5 mM stock solutions of the amino acids and peptides in deionized water were stored at 4 °C. For CE measurements, respective amounts of the stock solutions were pipetted into CE sample glass vials and diluted with deionized water to a final sample volume of 2 mL and to sample concentrations varying from 60 to 5,000 µM. Sodium tetraborate and sodium phosphate were tested as buffer substances for CZE separations of the biomolecules. For the borate buffer a 28 mM stock solution (pH 8.5, HPCE grade) from Fluka, Buchs, Switzerland, was diluted with deionized water up to 10 mM. The phosphate buffer was prepared by dissolving varying amounts of sodium dihydrogenphosphate (≥99.0 %, Sigma-Aldrich, Steinheim, Germany) in deionized water to reach phosphate concentrations between 10 and 100 mM and by adjusting a pH value of 6.5–9.0 with 1 M sodium hydroxide (prepared from p. a. quality pellets, Lachema, Brno, Czech Republic). The completed buffer solutions were vacuum filtrated over cellulose acetate membrane filters (0.45 µm pore size, from Whatman, Dassel, Germany), degassed in an ultrasonic bath for 10 min, and stored at 4 °C in glass flasks. Prior to use for CE measurements, the vials filled with 2 mL of the running buffer were degassed again for 5 min. During CE measurement series, the buffer solutions were renewed after three or four sample runs each.

The heavy metals Mn, Ni, and Co were employed in its divalent form as nitrate salts (1 g L^{-1} stock solutions from Merck). Solid Cu(II) chloride dihydrate (≥99 %) and Zn(II) chloride (≥98 %) (both from Fluka, Buchs, Switzerland) were weighed and dissolved in deionized water to make 1 mM stock solutions.

The biomolecules mentioned above were incubated with the heavy metals in varied molar ratios in deionized water for 15 min before injection into the CE capillary. In some samples precipitates were formed after metal incubation of the biomolecules that were removed before injection into the CE capillary by means of centrifugation at 10,000×*g* for 5 min (Heraeus Biofuge Primo R centrifuge, Thermo Scientific).

Capillary Electrophoretic Equipment

Two unmodified fused silica capillaries (72 cm effective length, 80.5 cm total length, 75 µm i.d., 365 µm o.d.): the first one characterized by an unextended detection window and the second one equipped with an extended light path called bubble cell were employed. Both capillary types were purchased from Agilent Technologies, Waldbronn, Germany. The CE measurements were performed with a HP 3D capillary electrophoresis system from Agilent Technologies, equipped with a diode array detector. Before first use and after longer storage times, the capillary was equilibrated using the following equilibration program: (1) flushing with H_2O for 84 s; (2) flushing with 0.1 M NaOH for 600 s; (3) flushing with running buffer for 300 s; (4) applying +30 kV for 300 s with running buffer at inlet and outlet electrode; (5) applying +20 kV for 1,200 s with running buffer at inlet and outlet electrode. The capillary was preconditioned before each sample injection by flushing with running buffer for 180 s and by applying a voltage of +20 kV for 500 s with running buffer at inlet and outlet electrode and flushed after each sample run with 0.1 M NaOH for 240 s and subsequently with running buffer for 180 s. All flushing steps were performed at a pressure of 940 mbar. Samples were injected hydrodynamically at 50 mbar × 10 s. The temperature of the capillary cassette was set to 20 °C. A separation voltage of +30 kV was applied. The UV absorption was recorded at 192 nm.

Results and Discussion

Optimization of CZE Separation of Low-Molar Mass, Sulfur-Containing, Redox-Active Biomolecules

The CZE separation of six low-molar mass sulfur-containing biomolecules representing the reduced and oxidized states of the amino acids cysteine and methionine as well as of the tripeptide glutathione using a fused silica capillary with an effective length of 72 cm was optimized by varying the type, the concentration, and the pH value of the separation buffer. Sodium phosphate and borate were tested in a concentration range between 10 and 100 mM (Fig. 1) and in a neutral to weakly alkaline range (pH values between 6.5 and 9.0) in order to approximate physiological conditions (Figs. 1c, 2). Using borate as background electrolyte, fronting peaks occurred for GSH and GSSG (Fig. 1a). Significant concentrations of the analyte influence the conductivity of the background electrolyte (BGE) that can no longer be regarded as constant. The resulting electromigration dispersion causes a characteristic triangular deformation of analyte peaks [23]. In CZE systems with weak electrolytes, pH effects lead to electromigration dispersion in addition to conductivity effects [24]. During the electrophoretic process, concentration discontinuities often form moving electrophoretic boundaries [25]. If no self-sharpening conditions for a pair of adjacent zones are reached, e.g. for BGE zone and a mixed zone involving BGE and analyte in a certain concentration ratio, an unsteady-state boundary evolves which shows electromigration dispersion [25]. Peak resolution and separation efficiency are unfavorably affected if a peak fronting occurs. Since the separation plate height increases with analyte dispersion, a smaller

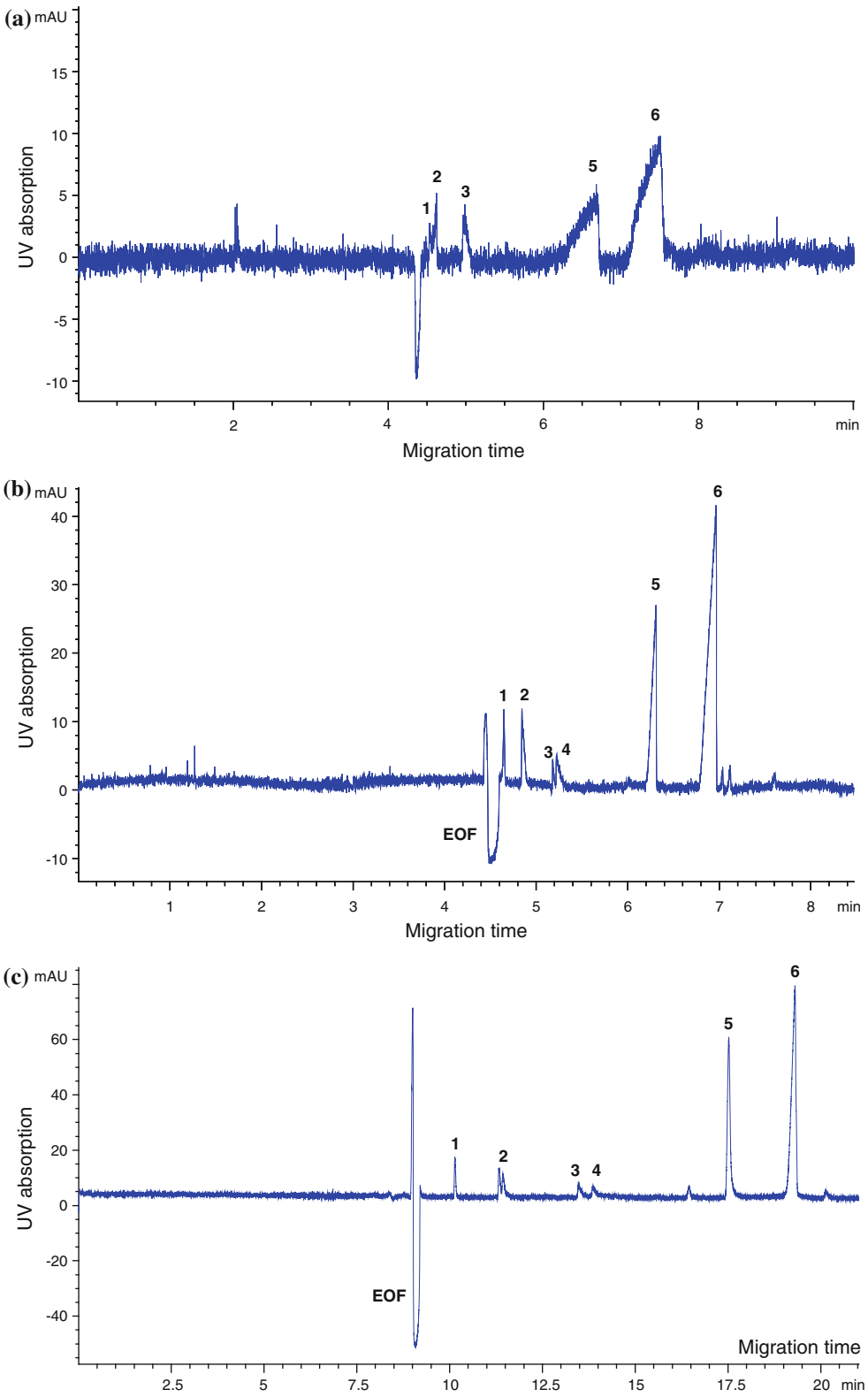

Fig. 1 Variation of the buffer type (**a** 10 mM borate, **b** 10 mM phosphate) and of the buffer concentration (**c** 100 mM phosphate) for the separation of the amino acids methionine (*1*), methionine sulfoxide (*2*), cysteine (*3*), cystine (*4*) and of the peptides glutathione (*5*) and glutathione disulfide (*6*) at pH 8.0 and +30 kV in a 75 µm i.d. fused silica capillary. Biomolecule concentration: 400 µM each (**a**, **b**), 800 µM each (**c**). Sample injection: 50 mbar × 10 s. Electric current: 10 µA (**a**), 14.5 µA (**b**), 100 µA (**c**). Data collection of UV detector: peakwidth <0.01 min, response time 0.1 s

separation plate number results at same separation distance [23]. Moreover, a lower detection sensitivity for the analytes resulted with the borate buffer compared to the phosphate buffer (Fig. 1a, b). The separation efficiency is improved with rising buffer concentration, because the biomolecules migrate slower due to diminished electrophoretic mobilities. With rising pH values in the background electrolyte, the migration time of the analytes

increased since they bear a stronger negative charge. Peak shapes of analytes change with pH and concentration of the BGE [26]. From the electropherograms arranged in Figs. 1 and 2, 100 mM sodium phosphate buffer, pH 8.0 can be concluded as optimum CZE separation condition. The most sensitive detection wavelength of 192 nm was deduced from a wavelength scan over the whole light emission spectrum of the deuterium lamp from $\lambda = 190$–600 nm using the diode array detector on-capillary. Further optimization parameters were the analyte concentrations in the samples for performing metal interaction studies. Sample concentrations of 800 µM for the peptides and of 3 mM for the amino acids provided the best evaluable electropherograms concerning both peak areas and resolution using the capillary with the unextended detection window. Therewith, biologically relevant concentrations of the biomolecules were analyzed (compare the GSH and Cys concentrations in hepatocytes mentioned in the "Introduction").

Figures of merit for the quantitative analysis of reduced and oxidized forms of the considered biomolecules under optimized CZE conditions are summarized in Table 1. The corrected peak areas are characterized by somewhat larger RSD values compared to the migration times but good repeatabilities of both parameters resulted. Good linearities of the recorded calibration lines demonstrate the suitability of the new method to carry out quantitative metal interaction studies. Limits of detection obtained by the 75 µm i.d. capillary could be improved by a factor of about 4 for the peptides characterized by larger molar UV absorptivities whereas detection limits of the smaller amino acids were two- to threefold enhanced. The double peak appearing for MetSO in the electropherograms (Figs. 1c, 2a) can be tentatively assigned to the two forms of oxidized

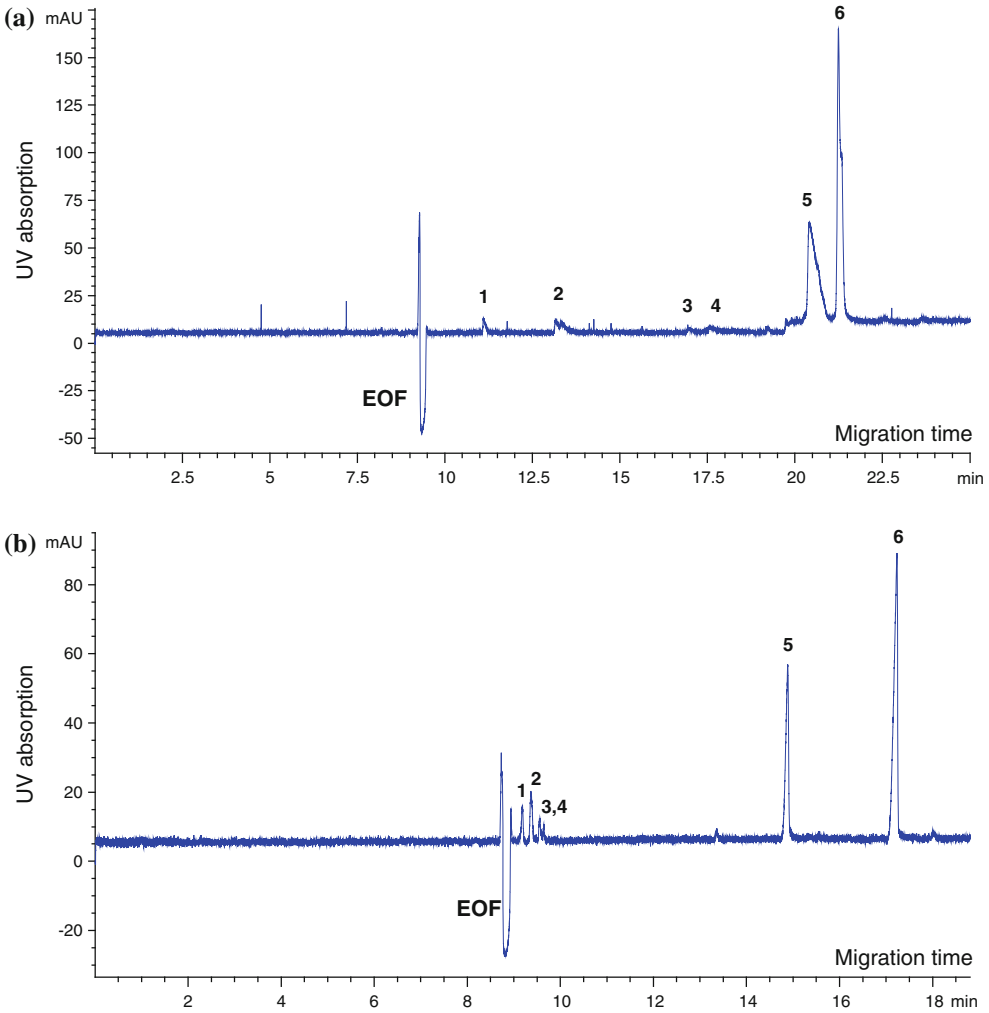

Fig. 2 Effect of the pH value of the 100 mM phosphate separation buffer on the CZE separation of six sulfur-containing, redox-active amino acids and peptides in a 75 µm i.d. fused silica capillary at +30 kV. **a** pH = 9.0, **b** pH = 6.5, 8.0 see Fig. 1c. Biomolecule concentration: 800 µM each. Sample injection: 50 mbar × 10 s. Electric current: 100 µA. Data collection of UV detector: peakwidth <0.01 min, response time 0.1 s

methionine, the sulfoxide, and the sulfone, that reflect successive oxidation states. For validation of analytical results presented in Table 1, the areas of both peaks were summed up.

Capillary Electrophoretic Evaluation of Heavy Metal Interactions with Sulfur-Containing, Redox-Active Amino Acids and Peptides

For CE studies of metal interactions with sulfur-containing, redox-active amino acids and peptides, the optimized separation conditions were chosen (100 mM phosphate buffer, pH 8.0, +30 kV). For the metal concentrations considered in the following experiments, the detection capability of the capillary with the unextended light path sufficed to detect the reduced and oxidized forms of the biomolecules if the initial biomolecule concentrations of 800 and 3,000 µM were chosen (see previous section). In order to analyze higher molar ratios of metal to biomolecule or lower initial biomolecule molarities, the capillary with the extended light path should be employed. Both migration times and peak areas of Met, MetSO, Cys–Cys, and GSSG did not change after incubation with Cu(II) and Zn(II) ions. In contrast to these findings, Cu(II) and Zn(II) complexes of methionine have been detected by means of potentiometric titrations [27, 28] as well as by nuclear magnetic resonance spectroscopy [28, 29]. The amino acid cysteine in its reduced form reacted both with Cu(II) and Zn(II), whereas reduced glutathione reacted with Cu(II) and Co(II) but not with Zn(II), Ni(II), and Mn(II).

The peak areas of the reduced biomolecules decreased with increasing metal concentrations, whereas the peak areas of the corresponding disulfides increased simultaneously (Fig. 3) indicating the following redox reactions:

$$2\,\text{Cys-SH} + \text{Me}^{2+} \rightleftharpoons \text{Cys-S-S-Cys} + \text{Me}^{0} + 2\text{H}^{+} \quad (1a)$$

$$\text{or } 2\,\text{Cys-SH} + 2\,\text{Me}^{2+} \rightleftharpoons \text{Cys-S-S-Cys} + 2\,\text{Me}^{1+} + 2\text{H}^{+} \quad (1b)$$

$$2\,\text{GSH} + \text{Me}^{2+} \rightleftharpoons \text{GSSG} + \text{Me}^{0} + 2\text{H}^{+} \quad (2a)$$

$$\text{or } 2\,\text{GSH} + 2\,\text{Me}^{2+} \rightleftharpoons \text{GSSG} + 2\,\text{Me}^{1+} + 2\text{H}^{+} \quad (2b)$$

For Cu(II) ions, the reactions described both in Eqs. 1a, 1b, and 2a, 2b are likely to take place because the Cu(I) ion can occur in aqueous solutions, whereas for the other considered metals (Zn, Co, Mn, Ni) the variants described in Eqs. 1a and 2a can be expected.

In case of Zn additions, Cys oxidation could be noticed at larger metal concentrations compared to Cu addition and the Cys peak area declined slower with increasing metal amounts (compare Fig. 4a, b). No cystine peak appeared in the electropherograms. We assume that the cystine concentrations were below the detection limit (338 µM, see Table 1) in case of the lower Zn amounts in the samples. A precipitate became visible from a Zn/amino acid ratio of 0.33:1. At this point, from the Cys peak area a Cys–Cys concentration of 360 µM can be concluded which is located near the detection limit and which is smaller than the solubility limit of cystine in water (792 µM). Possibly, larger Zn amounts reduce the cystine solubility owing to

Table 1 Validation results of the new CZE separation method for six low-molar mass, sulfur-containing biomolecules

Analyte	Intra-day repeatability (%)		Inter-day repeatability (%)	Linearity of calibration line				Limits of detection (µM)	
	Of migration time	Of corrected peak area	Of corrected peak area	75 µm i.d. capillary		Bubble cell capillary		75 µm i.d. capillary	Bubble cell capillary
				Concentration range	R^2	Concentration range	R^2		
Cysteine	1.66	3.9	4.2	400–4,000	0.982	250–1,500	0.974	366	118
Methionine	1.71	2.2	3.1	250–2,500	0.992	75–500	0.991	235	98
Glutathione	2.72	7.4	5.2	125–5,000	0.998	60–160	0.985	65	17
Cystine	1.83	4.2	6.7	400–800	0.997	200–700	0.973	338	154
Methionine sulfoxide	1.69	7.2	7.3	200–2,000	0.974	100–1,000	0.982	194	57
Glutathione disulfide	3.55	11.4	12.3	100–4,000	0.997	60–160	0.979	78	20

Intra-day repeatability expressed as relative standard deviation (RSD) was determined from five repeated measurements of the same sample containing 800 µM of each analyte. Inter-day repeatability was obtained from 3 days for freshly prepared samples containing 800 µM of each analyte. Calibration lines were recorded using four to six concentration levels per analyte. Detection limits were derived from the calibration lines by inserting the y axis intercept y_b and the corresponding standard deviation s_b in the equation for calculation of the peak area at the detection limit $y_{LOD} = y_b + 3s_b$. The corresponding concentration c_{LOD} was calculated according to the following equation with b denoting the slope of the calibration line: $c_{LOD} = (y_{LOD} - y_b)/b$

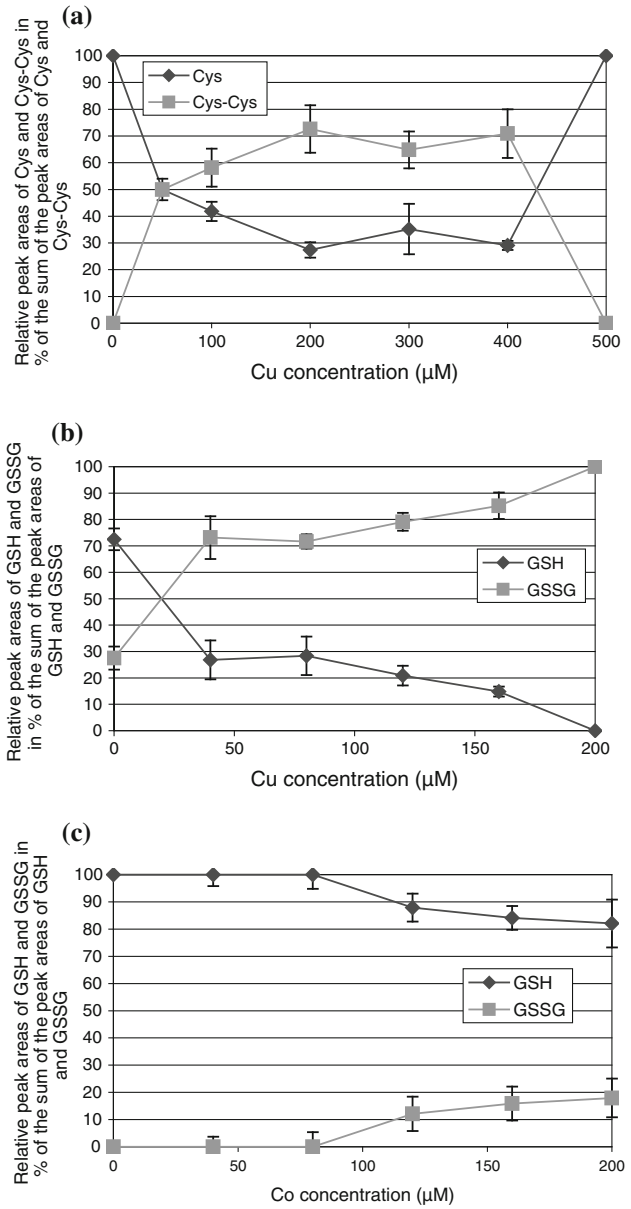

Fig. 3 Relative peak areas of the reduced and oxidized forms of cysteine (Cys and Cys–Cys) (**a**) and of glutathione (GSH and GSSG) (**b**, **c**) measured by CZE in dependent on the metal concentrations (Cu **a**, **b** and Zn **c**) incubated with the biomolecules. Initial concentrations of reduced biomolecules: 3,000 μM (Cys, **a**) and 800 μM (GSH **b**, **c**). Average values with standard deviations from $n = 3$ parallel samples are shown

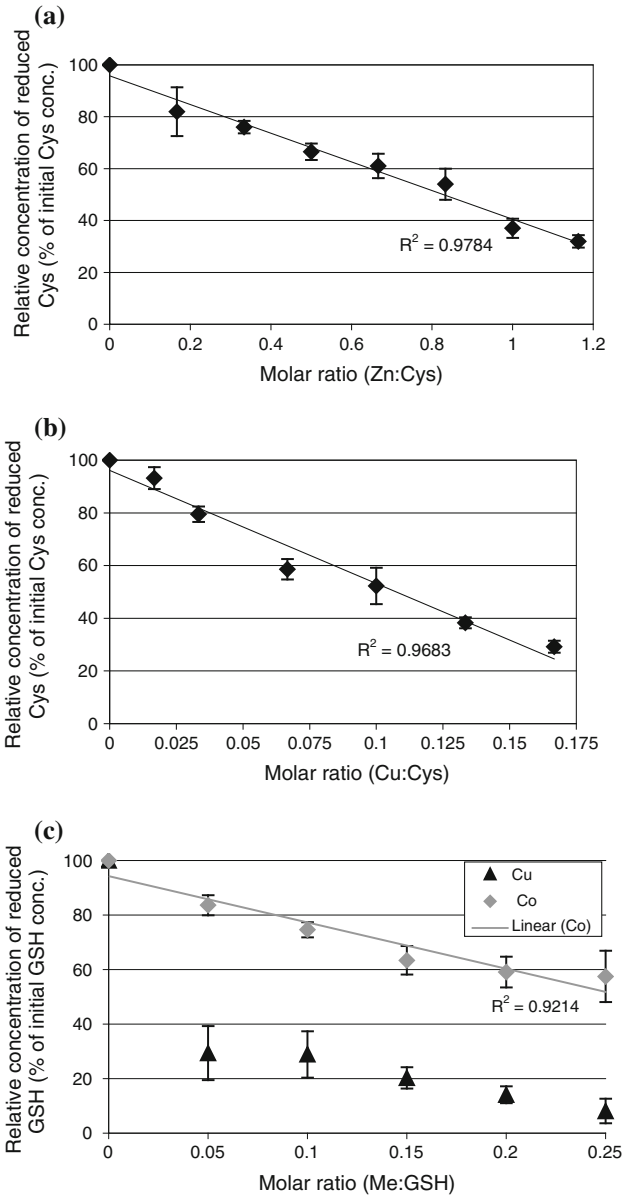

Fig. 4 Oxidation grade of cysteine (**a**, **b**) and glutathione (**c**) caused by heavy metals expressed as relative concentration of the reduced amino acid and peptide form. Initial concentration of Cys = 3,000 μM and of GSH = 800 μM. Calculation of the Cys and GSH concentration in dependent on the metal concentration from the peak areas obtained by CZE from $n = 3$ parallel samples

co-precipitation effects with $Zn^0_{(s)}$. In general, a narrow linear range for the dependence of the UV absorption on the molarity exists in case of cystine (Table 1).

The decrease of the reduced form of the amino acid caused by Cu(II) and Zn(II) ions showed a good linearity: $R^2 = 0.97$ for the Cu/Cys system; $R^2 = 0.98$ for the Zn/Cys system (Fig. 4a, b). Even though Cu was added to the Cys solution in a large stoichiometric deficiency, thiol oxidation can already be observed at a 60-fold molar Cys excess corresponding to a molar ratio of Cu:Cys = 0.017. Firstly, the cystine peak growed but due to a poor solubility in water (792 μM) this disulfidic dimer precipitated leading to a stagnating peak area around the solubility limit and finally up to a disappearance of the peak at Cu concentrations larger than 400 μM (Fig. 3a). For example, if 200 μM Cu are present in the cysteine sample, the peak area measured by CE corresponds to 1.56 mM of the reduced form of the amino acid so that 720 μM of cystine

has been formed. At the next experimental point (300 μM Cu), the Cys peak area indicates a cystine concentration of 800 μM exceeding the solubility limit. Cysteine concentrations were calculated by means of the calibration lines listed in Table 1. The Cys–Cys concentration was calculated by subtraction of the measured Cys concentration from the initial Cys concentration which was incubated with the metal and by subsequent division by a factor of 2 since two Cys molecules form one Cys–Cys molecule (Eq. 1a, 1b). This way of calculation was favored over the use of the cystine calibration listed in Table 1 because of the not predictable influence of solubility effects on cystine peak area. Possibly due to co-precipitation effects during the centrifugation step, the cystine peak disappeared below the detection limit with rising Cu concentrations similar to the assumed Zn(0)-cystine co-precipitations. Owing to the mentioned precipitate formations that also occurred in case of the GSH/GSSG system (see below), the disulfidic forms are not suited for the quantitative evaluation of the oxidation grade of the biomolecules. Therefore, the decreasing peak areas of the reduced forms were used for calculation of the oxidation grade (Eq. 3a, 3b; Fig. 4). The linear calibration lines mentioned in the previous section (optimization of CZE separation of low-molar mass, sulfur-containing, redox-active biomolecules) were used to calculate the GSH and Cys concentrations from the corresponding CZE peak areas.

$$[\mathrm{GSH}]_{\mathrm{ox}} = 0.5\,[\mathrm{GSSG}] = [\mathrm{GSH}]_0 - [\mathrm{GSH}]_{\text{measured by CZE in dependent on the metal conc.}} \quad (3a)$$

$$\text{Oxidation grade} = [\mathrm{GSH}]_{\mathrm{ox}} \times 100\%/[\mathrm{GSH}]_0. \quad (3b)$$

As mentioned above, both Zn(II) and Ni(II) ions did not affect the redox state of GSH. After incubation with stoichiometric deficiencies as well as with equimolar amounts of Zn or Ni, both peak area and migration time of the reduced tripeptide remained unchanged. The oxidation potential of Zn(II) ($E^{\theta}_{\mathrm{Zn(0)/Zn(II)}} = -0.7628$ V) is not sufficient to oxidize GSH ($E^{\theta}_{\mathrm{GSH/GSSG}} = -0.240$ V). This finding agrees with mass spectrometric Cu and Zn binding studies of GSH [9]. The standard redox potential of the Ni(0)/Ni(II) redox pair ($E^{\theta}_{\mathrm{Ni(0)/Ni(II)}} = -0.236$ V) resembles the potential of GSH/GSSG. A complex formation between reduced GSH and Zn(II) or Ni(II) ions occurs at pH values >10, if SH– and CO–NH-groups are deprotonated [30]. CE analysis in such alkaline media is not possible because metal hydroxides clog the capillary. Despite a somewhat higher redox potential of the GSH/GSSG system compared to the Co(0)/Co(II) redox pair ($E^{\theta}_{\mathrm{Co(0)/Co(II)}} = -0.282$ V), a slight decrease of the GSH peak area accompanied by an increasing GSSG peak area was observed (Fig. 3c). This could be ascribed to the concentration ratios of the oxidized and reduced forms of both the metal and the peptide that influence the potential of the complete redox reaction. The standard redox potentials are valid for standard concentrations defined to 1 mol L^{-1} of both the reduced and oxidized species of a redox pair. Moreover, solubility equilibria as well as the pH conditions affect the redox reactions. After incubation of GSH with Mn(II) which is characterized by a lower redox potential ($E^{\theta}_{\mathrm{Mn(0)(Mn(II)}} = -1.182$ V) compared to the peptide, both the migration time and the peak area of GSH remained unchanged but an additional peak occurred at $t_{\mathrm{M}} < t_{\mathrm{M,\ GSH}}$ which was characterized by an increasing area with rising Mn molarity. Because of the constant GSH peak area this peak can possibly be assigned to a Mn species.

A definite change of the GSH/GSSG ratio up to a decline of the GSH peak below the detection limit was recorded in case of Cu(II) addition to GSH in stoichiometric deficiency (Fig. 3b). At larger Cu molarities (Cu:GSH = 0.5, 0.625, 0.75, 0.875, and 1.0), the electropherograms altered. The GSSG peak completely disappeared presumably owing to precipitate formation (a white precipitate was observed) whereas a new peak appeared at a position of 18 min in the 72 cm long capillary between the migration times of GSH and GSSG. This peak exhibited a broad plateau at its front side. In another work [31], a Cu(II)-GSSG complex as well as a Cu(I)-GSH complex have been described. Since the former complex between the oxidized Cu and the oxidized glutathione is stable under neutral and alkaline conditions, the new peak can potentially be ascribed to this structure.

For the systems Cys + Zn, Cys + Cu, GSH + Cu, and GSH + Co, the 50 % oxidation grade of the biomolecule can be compared from the data shown in Fig. 4a–c. For Cu(II) caused oxidations, a 50 % oxidation grade was achieved at a molar ratio of Cu to GSH of 0.036 whereas a threefold larger molar ratio (Cu:Cys = 0.11) was necessary for 50 % Cys oxidation. 50 % of the initial Cys amount was oxidized by Zn(II) at a 7.7-fold larger molar Zn:Cys ratio (0.85) compared to the Cu(II) caused Cys oxidation. In case of the Co+GSH system, a 50 % oxidation grade of GSH was not achieved at the tested Co concentrations. A molar Co:GSH ratio of ≫0.25 can be assumed from Fig. 4c. According to Eq. 1a and 2a, the maximum concentration of oxidized Cys or GSH corresponds to the twofold metal concentration. This maximum oxidation grade of the biomolecule is achieved at a complete reaction degree of the applied metal amount. Factors calculated by division of the concentration of the oxidized Cys or GSH (determined from CZE measurements according to Eq. 3a) by the maximally possible concentration of oxidized Cys or GSH showed an increasing trend with rising molar excess of the biomolecules to the metals (Fig. 5). This confirms an expected rising metal reduction

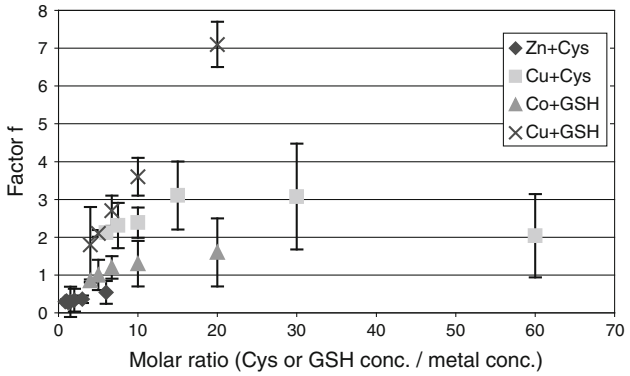

Fig. 5 Factors f determined by division of the concentration of oxidized Cys or GSH measured by CZE through the maximally possible concentration of oxidized Cys or GSH in dependent on the molar ratio of the biomolecule to the metal. Average values and standard deviations from $n = 3$ parallel samples are shown

grade with rising biomolecule concentration. Only in case of the Zn/Cys system, the maximum biomolecule oxidation was not achieved indicating an incomplete reduction of the applied Zn(II) amounts. A nearly complete Co(II) reduction can be assumed for the larger GSH molarities of the Co/GSH system, because the factors range around 1. In case of CZE measurements of the Cu-containing samples, the maximally possible concentrations of the oxidized forms of the biomolecules have been exceeded. The reason for this finding can be ascribed to an underestimation of the reduced Cys and GSH species by CZE measurements likely since the high oxidation grade of both biomolecules caused a pronounced precipitation of the disulfides as mentioned above which is presumably accompanied by a co-precipitation of the reduced forms. This experimental circumstance causes an error source for the metal interaction studies regarding a quantitative evaluation of CZE data especially in case of interaction systems containing metals with a large oxidation potential, such as copper. It is difficult to predict a concentration range for the analytes in which an exact quantification of the biomolecule oxidation by means of CZE is ensured since possible precipitation effects strongly depend on the type of metal as well as on the concentration ratios chosen. In order to validate the obtained CZE data, we therefore suggest the calculation of factors reflecting the ratio of the concentration of the oxidized biomolecule species obtained from CZE measurements to the maximum concentration which is defined by the initial concentration of the reduced biomolecule (compare Fig. 5).

Conclusions

A simple, non-elaborate CZE-based analytical method for quantitative evaluation of metal-caused biological thiol oxidation has been developed. The oxidation grades of cysteine and glutathione presented in this work in dependent on the kind and concentration of different heavy metals (Cu, Zn, Co) belong to the first quantitative data concerning biological thiol oxidation. Therewith, the disturbing effects of heavy metals on the cellular redox regulation can be demonstrated by means of CZE measurements. A general problem of the CZE-based metal interaction studies exists in the occurrence of precipitation and co-precipitation effects that result in a disappearance of the peaks of the oxidized biomolecule species accompanied by an underestimation of the reduced forms in some cases. To characterize metal-induced thiol oxidations for smaller initial biomolecule concentrations or for larger molar metal/biomolecule ratios than studied in the current experiments, a capillary equipped with an extended light path can be recommended. Detection limits of reduced and oxidized biomolecules could be improved by factors of 2–4 by this type of capillary simultaneously providing a high linearity of the UV detection over a wide concentration range.

Acknowledgments The authors thank the German Research Foundation (Deutsche Forschungsgemeinschaft, DFG) for financial support.

References

1. Chen G, Zhang L, Wang J (2004) Talanta 64:1018–1023
2. Bald E, Glowacki R, Drzewoski J (2001) J Chromatogr A 913:319–329
3. Carru C, Zinellu A, Sotgia S, Marongiu G, Farina MG, Usai MF, Pes GM, Tadolini B, Deiana L (2003) J Chromatogr A 1017:233–238
4. Žunića G, Spasić S (2008) J Chromatogr B 873:70–76
5. Bellomo G, Vairetti M, Stivala L, Mirabelli F, Richelmi P, Orrenius S (1992) Proc Natl Acad Sci USA 89:4412–4416
6. Griffith OW (1981) J Biol Chem 256:4900–4904
7. Kaplowitz N, Aw TY, Ookhtens M (1985) Ann Rev Pharmacol Toxicol 25:715–744
8. Hayashi Y, Nakagawa C, Mutoh N, Isobe M, Gotoh T (1991) Biochem Cell Biol 69:115–121
9. Schmidt AC, Koppelt J, Neustadt M, Otto M (2007) Rapid Commun Mass Spectrom 21:153–163
10. Russell J, Rabenstein DL (1996) Anal Biochem 242:136–144
11. Ling BL, Baeyens WRG, Dewaele C (1991) Anal Chim Acta 255:283–288
12. Toyo'oka T (2009) J Chromatogr B 877:3318–3330
13. Poinsot V, Gavard P, Feurer B, Couderc F (2010) Electrophoresis 31:105–121
14. Kašička V (2010) Electrophoresis 31:122–146
15. Pérez-Rama M, Abalde J, Herrero C, Suárez C, Torres E (2009) J Sep Sci 32:2152–2158
16. Kuśmierek K, Chwatko G, Głowacki R, Kubalczyk P, Bald E (2011) J Chromatogr B 879:1290–1307
17. Zhao S, Huang Y, Ye F, Shi M, Liu YM (2010) J Chromatogr A 1217:5732–5736
18. Yeh CF, Jiang SJ, Hsi TS (2004) Anal Chim Acta 502:57–63
19. Ivanov AV, Luzyanin BP, Moskovtsev AA, Rotkina AS, Kubatiev AA (2011) J Anal Chem 66:317–321

20. Kubota H, Sato K, Yamada T, Maitani T (1998) J Chromatogr A 803:315–320
21. Law WS, Zhao JH, Li SFY (2005) Electrophoresis 26:3486–3494
22. Mrestani Y, Claussen Y, Neubert RHH (2004) Chromatographia 59:759–762
23. Gaš B, Kenndler E (2000) Electrophoresis 21:3888–3897
24. Jaroš M, Soga T, van de Goor T, Gaš B (2005) Electrophoresis 26:1948–1953
25. Gebauer P, Boček P (2005) Electrophoresis 26:453–462
26. Erny GL, Bergström ET, Goodall DM (2003) Anal Chem 75:5197–5206
27. Sajadi SAA (2010) Adv Biosci Biotechnol 1:55–59
28. Griesser R, Hayes MG, McCormick B, Prijs B, Sigel H (1971) Arch Biochem Biophys 144:628–635
29. McCormick DB, Sigel H, Wright LD (1969) Biochim Biophys Acta 184:318–328
30. Krezel A, Bal W (2004) Bioinorg Chem Appl 2:293–305
31. Krezel A, Bal W (1999) Acta Biochim Polon 46:567–580